



Electrochemical and Plasmon-induced Grafting of n-Dopable π -Conjugated Oligomers

Mathieu Bastide, Denis Frath, Sarra Gam-derouich, Jean-christophe Lacroix

► To cite this version:

Mathieu Bastide, Denis Frath, Sarra Gam-derouich, Jean-christophe Lacroix. Electrochemical and Plasmon-induced Grafting of n-Dopable π -Conjugated Oligomers. ChemElectroChem, 2021, 8 (13), pp.2512-2518. 10.1002/celc.202100563 . hal-03420968

HAL Id: hal-03420968

<https://hal.science/hal-03420968>

Submitted on 9 Nov 2021

HAL is a multi-disciplinary open access archive for the deposit and dissemination of scientific research documents, whether they are published or not. The documents may come from teaching and research institutions in France or abroad, or from public or private research centers.

L'archive ouverte pluridisciplinaire **HAL**, est destinée au dépôt et à la diffusion de documents scientifiques de niveau recherche, publiés ou non, émanant des établissements d'enseignement et de recherche français ou étrangers, des laboratoires publics ou privés.

DOI: 10.1002/celc.202100563

Article

Received: 26. April. 2021

Revised: 06. Juni 2021

Accepted Article published: 10. Juni 2021

Electrochemical and Plasmon-induced Grafting of n-Dopable π -Conjugated Oligomers

Mathieu Bastide,^[a] Dr. Denis Frath,^[a] Dr. Sarra Gam-Derouich^[a] and Prof. Jean-Christophe Lacroix^{0000-0002-7024-4452*}^[a]

[a] <orgName/>Université de Paris
 <orgDiv/>ITODYS, CNRS, UMR 7086
 <street/>15 rue J.-A. de Baïf, <postCode/>75205 <city/>Paris Cedex 13,
 <country/>France
 E-mail: lacroix@univ-paris-diderot.fr

<pict> Supporting information for this article is available on the WWW under
 <url><http://dx.doi.org/10.1002/celc.202100563></url>

<spi> An invited contribution to a joint Special Collection in memory of Prof. Jean-Michel Savéant

Electrodes are functionalized by electrochemical reduction of the diazonium cation from 4-(2,3-diethylthieno[3,4-b]pyrazine-5-yl)aniline with ultrathin organic layers incorporating thienopyrazine units. This layer can be n-doped while being covalently grafted to the surface. Moreover, it can be deposited onto gold nanoparticles (NPs) by plasmon-induced diazonium reduction, thanks to the transfer of hot electrons from the excited plasmonic NPs to the diazonium salt. This confirms that localized surface plasmon resonance can induce nanolocalized electrochemical reactions.

The functionalization of electrodes by the reduction of diazonium cations generated *in situ* from 4-(2,3-diethylthieno[3,4-b]pyrazine-5-yl)aniline has been investigated. The thienopyrazine unit of this molecule is a precursor of n-dopable π -conjugated oligomers. Electrochemical reduction of diazonium cation coats the electrode with organic layers. Raman, IR, and XPS analyses show that their composition corresponds to that of the starting monomer, while AFM scratching measurements indicate thicknesses below 10 nm. The electrochemical responses of various reversible redox couples on the modified electrodes show that the attached layer is insulating in the positive potential range but can be n-doped at negative potential and switches to a conductive state. Moreover, oligo(4-(2,3-diethylthieno[3,4-b]pyrazine-5-yl)phenyl) can be selectively grafted onto gold nanoparticles (AuNPs) by plasmon-induced diazonium reduction. A 10–20 nm-thick organic layer is easily grafted onto each gold nanoparticle by visible-light illumination in a few minutes without any reducing agent or molecular photocatalyst. This result is attributed to the transfer of hot electrons from the excited plasmonic NPs to the diazonium, confirms that localized surface plasmon resonance can induce nanolocalized electrochemical reactions, and contributes to the emerging field of “plasmonic electrochemistry”.

diazonium electroreduction

n-dopable π -conjugated oligomers

plasmonic electrochemistry

surface functionalization

thin films

1. Introduction

Coating surfaces with organic layer is of great interest in many fields, from smart surfaces^[1–3] to sensors^[4–6] or organic and molecular electronics.^[7–11] In these fields π -conjugated oligomers continue to be the focus of intensive scientific research due to their unique properties: tunable band gap, redox properties, and low cost.^[12–15] P-dopable conjugated oligomers are much more developed than n-dopable materials as they are usually more stable in their doped conducting states.^[16] Development of new n-dopable oligomers is a highly active research field as such materials are crucial in new organic solar cells incorporating non-fullerene acceptors.^[17] Among the many types of n-dopable π -conjugated

oligomers, those incorporating thienopyrazine units (scheme¹) are widely used.^[18,19] This monomer consists of a central thiophene unit bearing an electron-withdrawing pyrazine moiety attached on the C3 and C4 carbon atoms of the thiophene. Incorporation of this unit in oligomers has been used to tune the gap of π -conjugated materials and to develop stable n-dopable or ambipolar materials for optoelectronic applications.^[20--24]

Π -conjugated oligomers can be deposited by various techniques, amongst which electrochemical oxidation of a monomer has been widely used. In this case, the bond between the substrate and the oligomers deposited is not covalent and the interface is often ill-defined. This drawback can be overcome by using the electrochemical reduction of diazonium salts, as it allows to graft adhesion primers or oligomers on the surface of the electrode by covalent bonds.^[25--30] This process generates nitrogen and highly reactive aromatic radicals in the vicinity of the electrode, whereupon the radicals react with the electrode leading to a bond at the interface.^[26,31] This reaction has been investigated on various materials such as metallic, diamond, carbon electrodes or semiconducting surfaces^[32--34] and in different media.^[35,36] Covalent bonding between the surface and the molecules was demonstrated by several experimental tools^[37--40] and indirectly evidenced by the strong adhesion, resisting sonication of the organic film that cannot be explained by weak interactions. The process usually generates ultrathin layers since the deposit is insulating in the potential range required for further electrochemical reduction of the diazonium salt. Such films are not well-defined single monolayers but multilayer films,^[41,42] consisting of disorganized oligomers, even though progress has been reported in this field.^[43--46]

Diazonium salts can be generated *in situ* from many amino aromatic precursors, and a wide variety, bearing various functionalities, has been used. When they incorporate thiophene,^[47,48] ethylenedioxythiophene,^[49] pyrrole^[50] or aniline^[27] moieties, π -conjugated oligomers, incorporating these electron-rich aromatic units, covalently grafted on surfaces, are

obtained. The grafted layers are electroactive at positive potential and the oligomers can be easily p-doped at potentials which depend on their molecular structure. As a consequence, all these layers show reversible on/off conductance switching at positive potential.^[51]

In this present work we wish to extend the variety of switchable conjugated oligomers that can be covalently grafted by diazonium reduction. We investigate the electroreduction of the diazonium salt derived from 4-(2,3-diethylthieno[3,4-b]pyrazine-5-yl)aniline, obtained in two steps from thienopyrazine (see scheme¹ for synthetic pathway). We show that this molecule can be grafted onto an electrode and characterize the modified surfaces by various techniques: IR, Raman, X-ray photoelectron (XPS) spectroscopies, AFM and electrochemistry. We show that on/off switching capabilities associated with oligo (thienopyrazine) materials are retained and that these oligomers can be also locally grafted onto gold nanoparticles by plasmon-induced diazonium reduction.^[52]

Experimental Section

Reagent-grade solvents and reagents were used as received from commercial sources unless specified otherwise. Thienopyrazine (TP) was synthesized according to the literature.^[53] Reactions were monitored by thin-layer chromatography (TLC silica gel 60^{F₂₅₄}). Column chromatography was performed using 40–63^{μm} silica gel and eluent mixtures are reported as volume ratios (v/v). ¹H and ¹³C NMR spectra were recorded on a Bruker AC400. ¹H and ¹³C chemical shifts are reported in parts per million (ppm) referenced to the residual non-deuterated solvent peak.

Synthesis of TP-NB

A solution of **TP** (300^{mg}) in dry THF (60^{mL}) under argon was cooled to <M>78^{°C}. BuLi (2.5^M, 0.75^{ml}, 1.87^{mmol}) was added and the mixture was stirred for 30^{minutes} at <M>78^{°C}. Bu₃SnCl (0.51^{ml}, 1.87^{mmol}) was added and the mixture was stirred for 30^{minutes} at <M>78^{°C} and for two hours at room temperature. Solvent was evaporated and the residue was

dissolved in toluene (30[^]mL). 1-Bromo-4-nitrobenzene (315[^]mg, 1.56[^]mmol) was added and the solution was degassed with argon. Pd(PPh₃)₄ was added and the solution was stirred at 90[^]°C for 18[^]h. It was then cooled to room temperature, washed with water and extracted with dichloromethane. Organic layers were dried over magnesium sulfate, evaporated, purified by silica gel chromatography eluted with dichloromethane/petroleum ether (9/1) and washed with pentane. Yield: 26[^]% (125[^]mg). ¹H NMR (400[^]MHz, CDCl₃) δ (ppm): 8.49 (2H, d, *J*=9.1[^]Hz, CH Arom), 8.30 (2H, q, *J*=9.1[^]Hz, CH Arom), 7.91 (1H, s, CH Arom), 3.01 (2H, q, *J*=7.3[^]Hz, CH₂ Ethyl), 2.96 (2H, q, *J*=7.3[^]Hz, CH₂ Ethyl), 1.47 (3H, t, *J*=7.2[^]Hz, CH₃ Ethyl), 1.40 (3H, t, *J*=7.2[^]Hz, CH₃ Ethyl).

Synthesis of TP-An

Hydrazine hydrate 60[^]% (0.27[^]ml) and Pd/C 10[^]% (32[^]mg, 0.031[^]mmol) were added to a solution of **TP-NB** (97[^]mg, 0.31[^]mmol) in THF (6[^]mL). The resulting mixture was refluxed for four hours. It was then evaporated and purified by silica gel chromatography eluted with dichloromethane. Yield: 65[^]% (57[^]mg). ¹H NMR (400.15[^]MHz, CD₃CN) δ (ppm): 7.97 (2H, d, *J*=8.8[^]Hz, CH Arom), 7.54 (1H, s, CH Arom), 6.73 (2H, d, *J*=8.8[^]Hz, CH Arom), 2.93 (2H, t, *J*=7.3[^]Hz, CH₂ Ethyl), 2.88 (2H, t, *J*=7.3[^]Hz, CH₂ Ethyl), 1.36 (3H, t, *J*=7.3[^]Hz, CH₃ Ethyl), 1.31 (3H, t, *J*=7.3[^]Hz, CH₃ Ethyl); ¹³C NMR (100.62[^]MHz, CD₃CN) δ (ppm): 158.6, 157.2, 149.4, 144.3, 130.1, 124.3, 115.8, 111.8, 29.3, 29.2, 11.91, 11.87; NMR spectra are given in the SI files as Figure[^]S1.

Electrochemical Experiments

A conventional three-electrode cell was used with a platinum wire as auxiliary electrode and a saturated calomel electrode (SCE) (3[^]M KCl) as reference. Three types of working electrode were used, namely glassy carbon (GC, 3[^]mm diameter), gold (1[^]cm²) for XPS and IR analysis, and plasmonic electrodes, i.e. ITO covered by gold nanoparticles or gold gratings, for surface-enhanced Raman spectroscopy. Before any measurements the solutions were deoxygenated by bubbling argon

for 30 min; during the experiment the electrochemical cell remained under argon. Electrochemical data were recorded on a CHI 660C potentiostat (CH Instruments, U.S.A.).

Infrared Reflection Absorption Spectroscopy (IRRAS)

IR spectra of a gold working electrode were recorded on a Nicolet Magna-IR 860 spectrometer with Fourier transform, equipped to measure the reflectivity under grazing incidence. IR spectra were referenced to that of a freshly cleaned gold surface.

Raman Spectroscopy

Raman spectra were recorded using an HORIBA Labram spectrometer with an excitation wavelength of 632 nm. Due to the lack of sensitivity, specific plasmonic electrodes were used. These substrates were obtained either by electrodeposition of gold nanoparticles (NPs) following an already published procedure^[54] or by e-beam lithography. In the last case, 100*100 μm arrays of spherical NPs were generated. The NPs are separated by 400 nm and each NP has a diameter of 120 nm. Procedures to generate such NPs have been reported elsewhere.^[55]

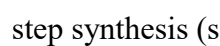

X-ray Photoelectron Spectroscopy

XPS analyses were performed on a modified gold substrate. The spectra was recorded using a K-Alpha system (Thermo Fishier Scientific, East-Grinstead , UK) fitted with a microfocused and monochromatic Al Ka X-ray beam (1486.6 eV, 400 μm spot size). The samples were stuck on sample holders using conductive double-sided adhesive. The surface composition was determined with version 5.9902 Advantage software by using the manufacturer sensitivity factors.

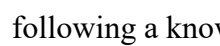
Atomic Force Microscopy

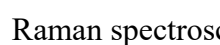
AFM measurements were performed using a Nano-Observer microscope (CSInstruments AFM Microscopes, France). Images were recorded in the tapping mode with a tip from Budgetsensor.

2. Results and Discussion

4-(2,3-Diethylthieno[3,4-b]pyrazine-5-yl)aniline (TP-C-An) was obtained by a two-step synthesis (scheme¹). The first step consists of a “one-pot” Stille coupling reaction with the non-isolated stannate intermediate to obtain the nitrobenzene derivative TP-NB in 26% yield. The second step is a Pd/C catalyzed reduction with hydrazine hydrate to form TP-C-An in 65% yield. Then, TP-C-An was used to modify the electrode surface by the electroreduction of the corresponding diazonium cation (TPP-N₂⁺). The diazonium salt was generated *in situ* and electrochemical grafting was carried out by cyclic voltammetry. Figure¹ shows the CV of the reduction on a GC electrode of TPP-N₂⁺ generated in acetonitrile containing 0.5 mmol.L⁻¹ of TP-C-An, 10 equivalents of tert-butyl nitrite and 0.1 M tetra-n-butylammonium tetrafluoroborate.

The recorded CV displays one irreversible reduction wave at ~ 0.14 V/SCE and a large reduction current from 0.0 to ~ 1.0 V. This behavior is associated with the reduction of TPP-N₂⁺. During subsequent cycles, the CV shows a significant decrease in the intensity of the reduction current, which disappears completely after 10 cycles. Similar behavior has been observed in the reduction of aryl diazonium cations generated *in situ*.^[31] It is attributed to the progressive modification of the electrode by the formation of an insulating organic film, which partially blocks the surface in the 0.0 to ~ 1.0 V potential range.

The thickness of the layer deposited was measured using the AFM scratch method following a known procedure.^[42] Figure¹ shows an image of a scratch made by the AFM tip. The depth of the hole is close to 5 to 6 nm, which is typically the result when insulating layers are generated by diazonium electroreduction in the potential range used.

The layers deposited on flat gold or plasmonic substrates were also analyzed by IR and Raman spectroscopy. Figure² shows the IR spectra of a film deposited on a gold

substrate while Figure² displays several Raman spectra of the starting precursor and of films generated on ITO or plasmonic electrodes.

The IR spectrum features bands at 2933 and 2953 cm^{-1} are attributed to the ethyl groups of the oligomers. Bands at 1606 and 1309 cm^{-1} originate from the pyrazine groups (C=C=N stretching and CH in-plane bending) while those at 1511 cm^{-1} and 1448 cm^{-1} reveal the presence of thiophene moieties^[56--58] Finally, C=C-H out-of-plane vibrations of the tetra- substituted pyrazine ring or 1,4-disubstituted phenyl moieties can be observed at 700 cm^{-1} and 800 cm^{-1} , respectively.

The Raman spectra of the same film deposited on ITO do not show any discernable signals while those recorded when the film is deposited on plasmonic electrodes (ITO bearing gold NPs) show several Raman shifts which are also observed in the spectra of TP-C-An (green curve). C=C=C and C=C=N shifts at 1600 cm^{-1} are very strong and indicate the presence of phenyl and pyrazine units on the surface.^[59] Raman shifts between 1400 and 1500 cm^{-1} can again be attributed to the thiophene rings^[60,61] while intense bands at 1275 and 1080 cm^{-1} are probably due to in-plane C=C-H bending of aromatic units known to be strong in Raman spectroscopy.

The grafted layers were also characterized by XPS. Comparison of the survey XPS spectra before and after grafting (Figure³) reveals several major changes. First the Au_{4f} (at 84 eV) signal is drastically attenuated, the carbon and nitrogen signals increase, then a new signal of sulfur appear after the reduction of the diazonium. The spectrum of a TPP sample shows strong C_{1s} and O_{1s} peaks at 285 and 532.7 eV, respectively, together with an N_{1s} peak at 400 eV and an S_{2p} sulfur signal at 164 eV, which indicates the formation of an organic layer. The relatively high O_{1s} signal indicates that the deposited layer seems sensitive to oxygen.

Figure³ shows the high-resolution C_{1s} XPS spectrum for the TPP sample, with a major peak at 285 eV and a second peak at 286.1 eV. The latter peak can be attributed to carbon atoms bonded to the nitrogens of the pyrazine moieties. The C₂₈₆/C₂₈₅ ratio is found to be 3.2 which is close to the theoretical ratio of 3.

Overall, AFM, IR Raman and XPS analysis confirm that an ultrathin film of oligo (TPP) can be easily be grafted onto gold, ITO and GC surfaces by diazonium electroreduction.

2.1. Electrochemical Characterization of the Grafted Layers

To study the electrochemical properties of the modified electrode, cyclic voltammetry was first used to test the blocking behavior of the electrode in the positive potential range. To do so the ferrocene redox couple was used. Figure⁴ shows the CV of this probe on a bare GC and a modified TPP/GC electrode. On the bare electrode there are the usual reversible Fc redox peaks centered on 0.3 V/ECS. These peaks are not observed on the TPP-modified electrode and are replaced by a small current plateau indicating a strong blocking effect of these films on Fc oxidation (with some micrometric holes sufficiently dispersed to be independent on the time-scale of the experiments^[62]). Sweeping the potential from -0.4 to 1.1 V also shows no electrochemical signal and underlines the strong homogeneity of the layer with no significant pinholes. This behavior is in marked contrast with those observed on grafted layers incorporating thiophene, pyrrole, EDOT or aniline.^[27,47--50,63] Indeed, on these electrodes the probe is irreversibly oxidized. This diode-like signal is the signature of a conductive switch of the grafted layer, and indicates that the oligomers can be p-doped at potentials below 1 V/SCE.

In a second step, we have used two different redox probes, namely 7,7,8,8-tetracyano-p-quinodimethane (TCNQ) and 4,4'-dimethylbipyridinium dichloride (VIO) known to be reversibly reduced in two successive one-electron processes on a bare electrode at different

potentials, (i.e. 0.2, -0.3 V/SCE for TCNQ and -0.4 and -0.8 V/SCE for VIO).

The two probes cannot be reduced at their usual reduction potentials, and the current is close to zero up to -1.5 V/SCE, which underlines the insulating behavior of the grafted layer in this potential window. However, a sharp irreversible reduction peak is observed for both probes at a very similar potential close to -1.7 V/SCE. The maximum current of these peaks reaches 110 μ A, which is more than twice that recorded on a bare electrode for each diffusion-limited monoelectronic reduction peak of TCNQ or VIO. These results indicate that the reduction of both probes is completely controlled by the electrochemical properties of the grafted TPP layer and that the layer can be n-doped at a potential close to -1.7 V/SCE and switches in a conductive state which makes reduction of the probes possible in a bi-electronic process. N-doping of the layer can also be evidenced by its electroactivity (Figure S2) observed at -1.7 V/SCE as a sharp reduction wave in a probe-free electrolyte (0.1 M solution of tetra-n-butylammonium tetrafluoroborate in acetonitrile). This behavior is close to that already observed by McCreery et al. with monolayers of biphenyl and nitrobiphenyl molecules.^[64] Note also that this behavior is not reversible as, after the reduction of the layer, TCNQ and VIO oxidation waves at potentials close to those for a bare electrode are partially recovered (Figure S3) during the reverse potential scan. This behavior can either be attributed to pinholes created in the TPP layer upon n doping or to oxygen induced degradation of the n-doped layer. Raman spectra (Figure 2b, blue curve) indicates that a film is still partially covering the gold nanoparticles after polarization below -1.7 V. Despite this drawback, TPP layers grafted by electrochemical reduction of thienopyrazine-phenyl diazonium cation appear to be n-dopable.^[65]

Next TPP grafting from diazonium solutions was triggered by localized surface plasmons. Previous works have shown that oligo(bisthienylbenzene) (BTB)^[66] and other aromatic units^[67] can be deposited onto gold nanoparticles (AuNPs) or in the gaps between gold NP dimers^[68] by visible-light illumination for a few minutes without any reducing agent or molecular photocatalyst. As grafting depends on the wavelength and polarization of the incident light, the orientation of the growth of the layer deposited on the AuNPs can be controlled. The mechanism of this plasmon-induced deposition process is considered to be the transfer of hot electrons from the excited plasmonic NPs to the diazonium salt, triggering the subsequent chemical reactions leading to surface modification.^[66--68]

Figure⁵ shows a scheme of the process. The plasmonic electrode used consists of $100 \times 100 \mu\text{m}^2$ arrays of spherical gold NPs (diameter 120 nm) with a 400 nm square grating deposited on ITO by e-beam lithography. It is fixed horizontally in a solution of acetonitrile containing 0.5 mmol.L^{-1} of TP-C-An, 10 equivalents of tert-butyl nitrite and 0.1 M tetra-n-butylammonium tetrafluoroborate, and is illuminated using white light from an optical microscope with a power of 0.54 W.cm^{-2} . Figure^{5b} shows an SEM image of the AuNPs after two minutes of irradiation (Figure^{S4} shows the SEM image of the AuNP before plasmon induced grafting for comparison purposes). One can see that a thin film (thickness around 10 nm) has been locally deposited on the AuNPs.

Figure^{5c} shows the Raman spectrum of the substrate for different positions. When the laser is focused on the ITO part of the electrode no Raman shift is recorded. On the contrary, an intense Raman spectrum is recorded when the laser is focused on the gratings. Raman shifts typical of pyrazine and thiophene groups show that the material deposited consists of oligo(TPP). Note also that some Raman shifts are strongly enhanced compared to those observed when the film is deposited by electrochemistry, which indicates that the orientation of the oligo(TPP) layer is not the same for both samples. (Orientational effects are

beyond the scope of the study and will be discussed elsewhere.) These results clearly demonstrate that oligo(TPP) can be locally grafted by light on a plasmonic substrate.

3. Conclusion

Electrodes have been functionalized by reduction of diazonium cation generated *in situ* from 4-(2,3-diethylthieno[3,4-*b*]pyrazine-5-yl)aniline. Electrochemical reduction of diazonium coats the electrode with ultrathin organic layers, consisting of aromatic oligomers and incorporating thienopyrazine units, a known building block for n-dopable π -conjugated oligomers. We show that this layer is insulating in the positive potential range and switches to a conductive state at negative potential, and can thus be n-doped while covalently grafted to the surface. Moreover, oligo(TPP) can also be selectively grafted onto gold NPs by plasmon-induced diazonium reduction. This result can be attributed to the transfer of hot electrons from the excited plasmonic NPs to the diazonium, and confirms that localized surface plasmon resonance can induce nanolocalized electrochemical reactions, thus contributing to the field of “plasmonic electrochemistry”.

Acknowledgements

The *Agence Nationale de la Recherche* (France ANR-19-APMJ) is gratefully acknowledged for its financial support for this work. The authors thank Mme S. Lau for Raman spectra and Dr. J. S. Lomas for English editing and scientific discussion. We also acknowledge the ITODYS SEM facility. This article is dedicated to Dr. Jean Michel Savéant for his great contribution in electrochemistry.

Conflict of Interest

The authors declare no conflict of interest.

- <lit1><book>A.[^]S.[^]H. Makhoulf, N.[^]Y. Abu-Thabit, *Advances in Smart Coatings and Thin Films for Future Industrial and Biomedical Engineering Applications*, Elsevier, **2019**</book>.
- <lit2><jnl>P. Nguyen-Tri, H.[^]N. Tran, C.[^]O. Plamondon, L. Tuduri, D.-V.[^]N. Vo, S. Nanda, A. Mishra, H.-P. Chao, A.[^]K. Bajpai, *Prog. Org. Coat.* **2019**, *132*, 235</jnl>.
- <lit3><jnl>L. Santos, J. Ghilane, J.[^]C. Lacroix, *J. Am. Chem. Soc.* **2012**, *134*, 5476</jnl>.
- <lit4><jnl>Y.[^]C. Wong, B.[^]C. Ang, A. Haseeb, A.[^]A. Baharuddin, Y.[^]H. Wong, *J. Electrochem. Soc.* **2019**, *167*, 37503</jnl>.
- <lit5><jnl>L. Kergoat, B. Piro, M. Berggren, G. Horowitz, M.-C. Pham, *Anal. Bioanal. Chem.* **2012**, *402*, 1813</jnl>.
- <lit6><jnl>J. Rivnay, S. Inal, A. Salleo, R.[^]M. Owens, M. Berggren, G.[^]G. Malliaras, *Nat. Rev. Mater.* **2018**, *3*, 1</jnl>.
- <lit7><jnl>Y. van[^]De[^]Burgt, A. Melianas, S.[^]T. Keene, G. Malliaras, A. Salleo, *Nat. Electron.* **2018**, *1*, 386</jnl>.
- <lit8><jnl>S. Casalini, C.[^]A. Bortolotti, F. Leonardi, F. Biscarini, *Chem. Soc. Rev.* **2017**, *46*, 40</jnl>.
- <lit9><jnl>A. Vilan, D. Aswal, D. Cahen, *Chem. Rev.* **2017**, *117*, 4248</jnl>.
- <lit10><jnl>H. Jeong, D. Kim, D. Xiang, T. Lee, *ACS Nano* **2017**, *11*, 6511</jnl>.
- <lit11><jnl>J.[^]C. Lacroix, *Curr. Opin. Electrochem.* **2018**, *7*, 153</jnl>.
- <lit12><jnl>K. Namsheer, C.[^]S. Rout, *RSC Adv.* **2021**, *11*, 5659</jnl>.
- <lit13><jnl>M. Talikowska, X. Fu, G. Lisak, *Biosens. Bioelectron.* **2019**, *135*, 50</jnl>.
- <lit14><jnl>S.[^]C. Rasmussen, *ChemPlusChem* **2020**, *85*, 1412</jnl>.

- <lit15><jnl>L. Ying, F. Huang, G. C. Bazan, *Nat. Commun.* **2017**, 8, 1</jnl>.
- <lit16><book>T. A. Skotheim, *Handbook of Conducting Polymers*, CRC Press, **1997**</book>.
- <lit17><jnl>C. Yan, S. Barlow, Z. Wang, H. Yan, A. K.-Y. Jen, S. R. Marder, X. Zhan, *Nat. Rev. Mater.* **2018**, 3, 1</jnl>.
- <lit18><jnl>J. Roncali, *Chem. Rev.* **1997**, 97, 173</jnl>.
- <lit19><jnl>S. Akoudad, J. Roncali, *Chem. Commun.* **1998**, 2081</jnl>.
- <lit20><jnl>R. S. Ashraf, M. Shahid, E. Klemm, M. Al-Ibrahim, S. Sensfuss, *Macromol. Rapid Commun.* **2006**, 27, 1454</jnl>.
- <lit21><jnl>A. P. Zoombelt, J. Gilot, M. M. Wienk, R. A. J. Janssen, *Chem. Mater.* **2009**, 21, 1663</jnl>.
- <lit22><jnl>H. Cheema, A. Peddapuram, R. E. Adams, L. McNamara, L. A. Hunt, N. Le, D. L. Watkins, N. I. Hammer, R. H. Schmehl, J. H. Delcamp, *J. Org. Chem.* **2017**, 82, 12038</jnl>.
- <lit23><jnl>M. J. Alonso-Navarro, A. Harbuzaru, P. de Echegaray, I. Arrechea-Marcos, A. Harillo-Baños, A. de la Peña, M. M. Ramos, J. T. López Navarrete, M. Campoy-Quiles, R. Ponce Ortiz, J. L. Segura, *J. Mater. Chem. C* **2020**, 8, 15277</jnl>.
- <lit24><jnl>P. Meti, H.-H. Park, Y.-D. Gong, *J. Mater. Chem. C* **2020**, 8, 352</jnl>.
- <lit25><jnl>J. Pinson, F. Podvorica, *Chem. Soc. Rev.* **2005**, 34, 429</jnl>.
- <lit26><jnl>S. Mahouche-Chergui, S. Gam-Derouich, C. Mangeney, M. M. Chehimi, *Chem. Soc. Rev.* **2011**, 40, 4143</jnl>.

- <lit27><jnl>L.[^]M. Santos, J. Ghilane, C. Fave, P.-C. Lacaze, H. Randriamahazaka, L.[^]M. Abrantes, J.-C. Lacroix, *J. Phys. Chem. C* **2008**, *112*, 16103</jnl>.
- <lit28><jnl>V. Stockhausen, V.[^]Q. Nguyen, P. Martin, J.[^]C. Lacroix, *ACS Appl. Mater. Interfaces* **2017**, *9*, 610</jnl>.
- <lit29><jnl>E. Villemin, B. Lemarque, T.[^]T. Vũ, V.[^]Q. Nguyen, G. Trippé-Allard, P. Martin, P.-C. Lacaze, J.-C. Lacroix, *Synth. Met.* **2019**, *248*, 45</jnl>.
- <lit30><jnl>M. Lo, R. Pires, K. Diaw, D. Gningue-Sall, M.[^]A. Oturan, J.-J. Aaron, M.[^]M. Chehimi, *Surfaces* **2018**, *1*, 43</jnl>.
- <lit31><jnl>D. Bélanger, J. Pinson, D. Belanger, J. Pinson, D. Bélanger, J. Pinson, *Chem. Soc. Rev.* **2011**, *40*, 3995</jnl>.
- <lit32><jnl>M.-C. Bernard, A. Chaussé, E. Cabet-Deliry, M.[^]M. Chehimi, J. Pinson, F. Podvorica, C. Vautrin-UI, *Chem. Mater.* **2003**, *15*, 3450</jnl>.
- <lit33><jnl>Y.[^]L. Zhong, K.[^]P. Loh, A. Midya, Z.-K. Chen, *Chem. Mater.* **2008**, *20*, 3137</jnl>.
- <lit34><jnl>S. Samanta, I. Bakas, A. Singh, D.[^]K. Aswal, M.[^]M. Chehimi, *Langmuir* **2014**, *30*, 9397</jnl>.
- <lit35><jnl>P.[^]A. Brooksby, A.[^]J. Downard, *Langmuir* **2004**, *20*, 5038</jnl>.
- <lit36><jnl>J. Ghilane, P. Martin, O. Fontaine, J.-C. Lacroix, H. Randriamahazaka, *Electrochem. Commun.* **2008**, *10*, 1060</jnl>.
- <lit37><jnl>D.[^]M. Shewchuk, M.[^]T. McDermott, *Langmuir* **2009**, *25*, 4556</jnl>.
- <lit38><jnl>L. Laurentius, S.[^]R. Stoyanov, S. Gusarov, A. Kovalenko, R. Du, G.[^]P. Lopinski, M.[^]T. McDermott, *ACS Nano* **2011**, *5*, 4219</jnl>.

- <lit39><jnl>J. Greenwood, T.[^]H. Phan, Y. Fujita, Z. Li, O. Ivasenko, W. Vanderlinden, H. Van[^]Gorp, W. Frederickx, G. Lu, K. Tahara, Y. Tobe, H. Uji-i, S.[^]F.[^]L. Mertens, S. De[^]Feyter, *ACS Nano* **2015**, *9*, 5520</jnl>.
- <lit40><jnl>H. Li, G. Kopiec, F. Müller, F. Nyßen, K. Shimizu, M. Ceccato, K. Daasbjerg, N. Plumeré, *JACS* **2021**, *1*, 362</jnl>.
- <lit41><jnl>T. Itoh, R.[^]L. McCreery, *J. Am. Chem. Soc.* **2002**, *124*, 10894</jnl>.
- <lit42><jnl>F. Anariba, S.[^]H. DuVall, R.[^]L. McCreery, *Anal. Chem.* **2003**, *75*, 3837</jnl>.
- <lit43><jnl>C. Combellas, F. Kanoufi, J. Pinson, F.[^]I. Podvorica, *J. Am. Chem. Soc.* **2008**, *130*, 8576</jnl>.
- <lit44><jnl>Y.[^]R. Leroux, H. Fei, J.-M. Noël, C. Roux, P. Hapiot, *J. Am. Chem. Soc.* **2010**, *132*, 14039</jnl>.
- <lit45><jnl>T. Menanteau, E. Levillain, T. Breton, *Chem. Mater.* **2013**, *25*, 2905</jnl>.
- <lit46><jnl>V.[^]Q. Nguyen, X. Sun, F. Lafalet, J.[^]F. Audibert, F. Miomandre, G. Lemerrier, F. Loiseau, J.[^]C. Lacroix, *J. Am. Chem. Soc.* **2016**, *138*, 9381</jnl>.
- <lit47><jnl>C. Fave, Y. Leroux, G. Trippé, H. Randriamahazaka, V. Noel, J.-C. Lacroix, G. Trippé, H. Randriamahazaka, V. Noel, J.-C. Lacroix, *J. Am. Chem. Soc.* **2007**, *129*, 1890</jnl>.
- <lit48><jnl>V. Stockhausen, J. Ghilane, P. Martin, G. Trippe-Allard, H. Randriamahazaka, J.[^]C. Lacroix, *J. Am. Chem. Soc.* **2009**, *131*, 14920</jnl>.
- <lit49><jnl>V. Stockhausen, G. Trippe-Allard, V.[^]Q. Nguyen, J. Ghilane, J.-C. Lacroix, *J. Phys. Chem. C* **2015**, *119*, 19218</jnl>.
- <lit50><jnl>T.[^]H. Le, V.[^]Q. Nguyen, G. Trippe-Allard, J.-C. Lacroix, P. Martin, *Electrochemistry* **2020**, *1*, 20</jnl>.

- <lit51><jnl>C. Fave, V. Noel, J. Ghilane, G. Trippé-Allard, H. Randriamahazaka, J.[^]C. Lacroix, *J. Phys. Chem. C* **2008**, *112*, 18638</jnl>.
- <lit52><jnl>J.-C. Lacroix, Q. van[^]Nguyen, Y. Ai, Q. van[^]Nguyen, P. Martin, P.-C. Lacaze, *Polym. Int.* **2019**, *68*, 607</jnl>.
- <lit53><jnl>L.[^]E. McNamara, N. Liyanage, A. Peddapuram, J.[^]S. Murphy, J.[^]H. Delcamp, N.[^]I. Hammer, *J. Org. Chem.* **2016**, *81*, 32</jnl>.
- <lit54><jnl>V.-Q. Nguyen, D. Schaming, P. Martin, J.-C. Lacroix, *Electrochim. Acta* **2015**, *179*, 282</jnl>.
- <lit55><jnl>Y.[^]R. Leroux, J.[^]C. Lacroix, K.[^]I. Chane-Ching, C. Fave, N. Félidj, G. Lévi, J. Aubard, J.[^]R. Krenn, A. Hohenau, *J. Am. Chem. Soc.* **2005**, *127*, 16022</jnl>.
- <lit56><jnl>Y. Furukawa, M. Akimoto, I. Harada, *Synth. Met.* **1987**, *18*, 151</jnl>.
- <lit57><jnl>C. Mangeney, J. Lacroix, K.[^]I. Chane-Ching, M. Jouini, F. Villain, S. Ammar, N. Jouini, P. Lacaze, *Chem. Eur. J.* **2001**, *7*, 5029</jnl>.
- <lit58><jnl>C. Mangeney, J.-C. Lacroix, K.[^]I. Chane-Ching, M. Jouini, S. Aeiyaach, P.-C. Lacaze, *Phys. Chem. Chem. Phys.* **1999**, *1*, 2755</jnl>.
- <lit59><jnl>J. Kastner, H. Kuzmany, D. Vegh, M. Landl, L. Cuff, M. Kertesz, *Synth. Met.* **1995**, *69*, 593</jnl>.
- <lit60><jnl>E.[^]A. Bazzaoui, G. Levi, S. Aeiyaach, J. Aubard, J.[^]P. Marsault, P.[^]C. Lacaze, *J. Phys. Chem.* **1995**, *99*, 6628</jnl>.
- <lit61><jnl>M.[^]S. Barclay, C.[^]G. Elles, M. Caricato, *J. Phys. Chem. A* **2020**, *124*, 4678</jnl>.
- <lit62><jnl>C. Amatore, J.[^]M. Savéant, D. Tessier, *J. Electroanal. Chem. Interfacial Electrochem.* **1983**, *147*, 39</jnl>.

<lit63><jnl>V. Stockhausen, V.^Q. Nguyen, P. Martin, J.^C. Lacroix, *ACS Appl. Mater. Interfaces* **2017**, 9, 610</jnl>.

<lit64><jnl>A.^O. Solak, L.^R. Eichorst, W.^J. Clark, R.^L. McCreery, *Anal. Chem.* **2003**, 75, 296</jnl>.

<lit65><jnl>J. Casado, R.^P. Ortiz, M.^C. Ruiz^{Delgado}, V. Hernández, J.^T. López^{Navarrete}, J.-M. Raimundo, P. Blanchard, M. Allain, J. Roncali, *J. Phys. Chem. B* **2005**, 109, 16616</jnl>.

<lit66><jnl>V.^Q. Nguyen, Y. Ai, P. Martin, J.^C. Lacroix, *ACS Omega* **2017**, 2, 1947</jnl>.

<lit67><jnl>M. Nguyen, I. Kherbouche, S. Gam-Derouich, I. Ragheb, S. Lau-Truong, A. Lamouri, G. Lévi, J. Aubard, P. Decorse, N. Félidj, C. Mangeney, *Chem. Commun.* **2017**, 53, 11364</jnl>.

<lit68><jnl>P. Bléteau, M. Bastide, S. Gam-Derouich, P. Martin, R. Bonnet, J.-C. Lacroix, *ACS Appl. Nano Mater.* **2020**, 3, 7789</jnl>.

Figure¹ (a) Cyclic voltammetry on a carbon electrode for the electroreduction of TPP-N₂⁺ generated in acetonitrile containing 0.5^{mmol.L}^{<M>1} of TP<C->An, 10 equivalents of tert-butyl nitrite and 0.1^M tetra-n-butylammonium tetrafluoroborate (15 cycles). Scan rate 0.1^{V.s}^{<M>1}. (b) Thickness measurement of an oligo(TPP) film deposited on an ITO electrode. Inset shows the scratch made by the tip.

Figure² IR and Raman characterization of the thin film generated by electroreduction of TPP-N₂⁺. (a) IRRAS of a film deposited on a gold mirror. (b) Raman spectra of the starting TP<C->An precursor (green curve), of a TPP film electrodeposited on an ITO electrode (black curve) and on a plasmonic electrode before (red curve) and after (blue curve) polarization at <M>2^{V/SCE}.

Figure³ (a) XPS survey spectra of the initial and the TTP-modified gold electrode. (b) High-resolution C_{1s} spectra.

Figure⁴ Electrochemical response of various electrochemical probes on a bare GC electrode (dotted lines) and on a TPP-modified GC electrode (plain lines) in 0.1 M solution of tetra-n-butylammonium tetrafluoroborate in acetonitrile. (a) Ferrocene (10^{-2} M). (b) TCNQ (5×10^{-3} M, blue curves) and VIO (5×10^{-3} M, red curves) electrochemical response on a bare electrode and on a TPP-modified electrode Scan rate 0.1 V.s⁻¹.

Figure⁵ (a) Scheme of the plasmon-induced grafting process on a gold array of spherical NPs. (b) SEM image showing AuNPs after illumination in a solution of acetonitrile containing 0.5 mmol.L⁻¹ of TP-C-An, 10 equivalents of tert-butyl nitrite and 0.1 M tetra-n-butylammonium tetrafluoroborate. Light illumination power: 0.54 W.cm⁻². (c) SERS spectrum of the organic material deposited on the arrays of AuNPs (blue curve). Raman spectrum recorded on the ITO surface (black curve), SERS spectrum of the starting TP-C-An precursor (green curve)

Figure⁴ a displays the electrochemical signal of these probes on a bare carbon electrode and on a TPP-modified carbon electrode.

Scheme¹ Synthetic pathway of 4-(2,3-diethylthieno[3,4-b]pyrazine-5-yl)aniline.